

Relaxation and fluctuations in glassy fast-ion conductors: Wide-frequency-range NMR and conductivity measurements

F. Borsa* and D. R. Torgeson

Ames Laboratory, Department of Physics and Astronomy, Iowa State University, Ames, Iowa 50011-3020

S. W. Martin and H. K. Patel

Department of Materials Science and Engineering, Iowa State University, Ames, Iowa 50011-3020

(Received 3 December 1991)

^7Li nuclear spin-lattice relaxation rates (R_1) versus the temperature at several resonance frequencies (4 to 40 MHz) are reported together with the conductivity measurements, $\sigma(\omega)$, in the range 1 Hz to 3.76 MHz on $0.56\text{Li}_2\text{S}+0.44\text{Si}_2\text{S}$, a glassy fast-ionic conductor. Both R_1 and $\sigma(\omega)$ are fitted consistently over the whole temperature and frequency range by using a stretched-exponential, i.e., $\exp(-t/\tau_c^*)^\beta$ for the corresponding correlation functions (CF). Formulas that relate $R_1(\omega)$ and $\sigma(\omega)$ and that give the asymptotic behavior as functions of T and ω of both quantities are tested experimentally. We find significant differences between β_σ related to $\sigma(\omega)$ and β_R related to R_1 , which implies a difference in the corresponding correlation functions of the ionic diffusional motion. An apparent order-of-magnitude difference in τ_0^* attempt times was derived from these conductivity and NMR measurements. The implications of these findings are discussed in terms of the microscopic mechanisms which lead to fluctuations and relaxation in fast-ionic conductors.

I. INTRODUCTION

The transport properties of fast-ion conductors (FIC) depend largely upon the hopping dynamics of ionic charge carriers. Although the motion of ionic charge carriers has been examined using many different techniques, the two techniques most widely used are NMR (Refs. 1 and 2) and conductivity measurements.³

The NMR spin-lattice relaxation rate (NSLR) R_1 is related to the spectral density of the position-position correlation function (CF) and thus probes the local charge-density fluctuations. The frequency-dependent conductivity, on the other hand, measures the macroscopic relaxation properties of the electric field and thus probes the dissipation due to the long-range diffusion of the charges.⁴

The correct comparison of the results obtained by the two techniques is of paramount importance for the understanding of the ionic transport dynamics from a microscopic point of view. The comparison of measured parameters, such as the activation energies, obtained from limited ranges of temperature and/or frequency has often led to discrepancies and ambiguous conclusions.² Indeed, to our knowledge there has been no previous report of measurements of both $\sigma(\omega)$ and R_1 on the same FIC system where the frequency dependence of both phenomena has been examined.² Previous reports at best show R_1 at multiple frequencies and compare these to σ_{dc} and have not attempted to fit wide-frequency-range measurements of both R_1 and $\sigma(\omega)$ to the same correlation function. Recently, it was suggested^{2,5} these discrepancies can be removed by comparing measurements of NMR relaxation and ac conductivity over a wide range of both temperature and measuring frequency.

The frequency dependence of the conductivity^{2,5} and the deviation from the ω^{-2} frequency dependence of the NSLR (Refs. 2 and 6) are both a consequence of the nonexponential behavior of the relevant correlation functions (CF). Nonexponentiality in the CF's has been the observation for nearly all fast-ion conducting (FIC) glasses and is most often interpreted as a result of correlation between the ions during diffusive motion. Only in the limit of nearly zero (ppm) ion concentration does exponential relaxation result. Nonexponentiality is often described by a time dependence of the form $\exp[-(t/\tau_c^*)^\beta]$, where $0 < \beta < 1$, known as the stretched-exponential or Kohlrausch-Williams-Watts (KWW) function.⁷ The physical significance of the KWW function is an important, but debated, question: It could be simply the indication of inhomogeneous relaxation, i.e., a distribution of correlation times^{2,8} or it could represent the more fundamental effect of the slowing down of the relaxation at long times due to cooperative effects.⁹

The scope of this work is, therefore, to examine the extent to which a universal description of the conductivity and NMR relaxation can be developed by properly accounting for the nonexponentiality of both processes. In doing this, it is essential to verify experimentally the relationship between the measurements of relaxation [$\sigma(\omega)$] and fluctuation (R_1) using the two different techniques on the same systems over wide ranges of temperatures and measuring frequencies. To this end, we have performed measurements of ^7Li spin-lattice relaxation rate and of dc and ac ionic conductivities in $\text{Li}_2\text{S}+\text{Si}_2\text{S}$ glassy superionic conductors.¹⁰ These systems have been chosen because of their high ionic conductivity⁵ of $\approx 10^{-3}$ (Ωcm)⁻¹ at room temperature. The maximum spin-lattice relaxation rate $R_1 = T_1^{-1}$ occurs at low enough temperature so that both the high- and low-temperature

sides of the relaxation rate maximum peak can be investigated as a function of measuring frequency and compared with the dc and ac ionic conductivities, respectively.

II. EXPERIMENTAL DETAILS

Glasses of variable composition, $0.40 \leq x\text{Li}_2\text{S} \leq 0.60$, were prepared in an O_2 - and H_2O -free glovebox by mixing in a mortar and pestle Li_2S (Cerac, 99.9%) and SiS_2 obtained by reacting Si (Alpha, 99.999%) and S (Alpha, 99.999%) in a sealed quartz ampule.¹¹ The mixture was melted in a covered vitreous carbon crucible at 1000°C in a Mo-wire-wound furnace for 5–10 min. and then quenched into a preheated stainless-steel mold. Samples for the ionic conductivity were sputtered with gold contacts and measured over the frequency range 1 Hz to 3.76 MHz and over the temperature range 100–500 K by using a Solatron 1240 analyzer and a home-built conductivity cell.¹² The dc conductivities were determined from complex impedance plane plots and the real part of the ac conductivity was determined from the frequency dependence of the impedance. Not only do the conductivity measurements yield the ac conductivity, but they also allow the determination of the dc conductivity in the presence of electrode polarization. Since it proves experimentally convenient to use gold contact electrodes, these electrodes do introduce the problem of electrode polarization due to the build up of Li^+ ion charge at the irreversible gold electrodes. This effect decreases the measured dc conductivity due to a decreased voltage across the sample. Complex plane analysis of the impedance, however, allows the dc conductivity to be determined even when severe electrode polarization is present.

The NMR samples were sealed under vacuum in quartz ampules and the ^7Li relaxation measurements were performed at 4, 7, 12.2, and 40 MHz over the temperature range 100–500 K using a phase-coherent pulse NMR spectrometer.¹³ The sample temperatures were varied by means of a variable temperature chamber with a vacuum jacketed counter-flow, heat exchanger design and a three-term temperature controller based on an Omega Engineering 2012 programmable temperature control system. An NMR inversion recovery rf pulse sequence of $\pi - \pi/2$ was used to measure R_1 . The ^7Li spectral line width changes as a function of temperature due to motional effects but the quadrupole effects remain small ($\nu_Q < 100$ kHz) so that both central line and satellite lines can be irradiated yielding an exponential recovery of the nuclear magnetization at all temperatures.

III. RESULTS AND DISCUSSION

The frequency and temperature dependence of the ionic conductivity are shown in Figs. 1(a), 1(b), and in Fig. 2. In Fig. 3 the ^7Li nuclear spin-lattice relaxation rates are plotted as functions of temperature at different frequencies and as functions of frequency at different temperature, respectively. The results agree well with results reported earlier.¹⁴

By comparing the frequency dependence of both phenomena, a number of theoretical predictions can be

developed. Consider first the spin-lattice relaxation rate that is related to the spectral density $J(\omega_L)$ of the fluctuations due to the Li^+ hopping motion:^{1,2}

$$R_1 = C[J(\omega_L) + 4J(2\omega_L)], \quad (1)$$

where

$$J(\omega_L) = \text{Re} \int_{-\infty}^{\infty} f(t) \exp(-i\omega_L t) dt$$

and $f(t)$ is the CF of local lattice variables.

Both nuclear-nuclear magnetic dipole interactions and nuclear-electric quadrupole interactions are expected to contribute to the coupling constant C . Since both interactions are modulated in time by the Li ions dynamics, the CF $f(t)$ describes the time decay of some lattice function due to the diffusion of Li^+ ions. If at the time $t \leq \omega_L^{-1}$, the CF has decayed essentially to zero, then one has from Eq. (1),

$$R_1 \propto J(0) = 2 \int_0^{\infty} f(t) dt \equiv 2\tau_{\text{eff}}. \quad (2)$$

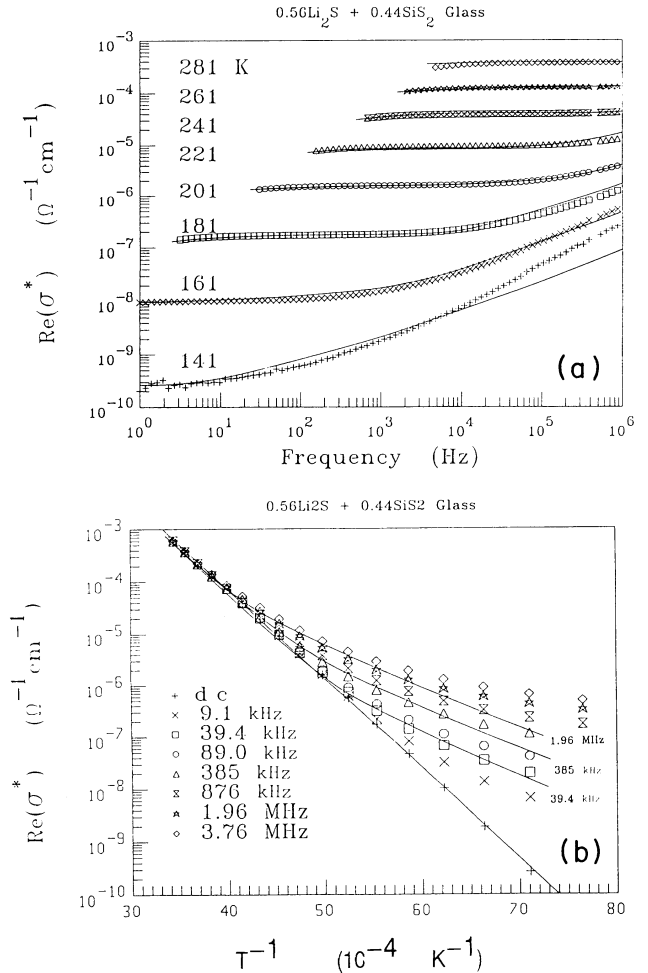


FIG. 1. (a) The real part of the measured ion conductivity of $0.56\text{Li}_2\text{S} + 0.44\text{SiS}_2$ vs measurement frequency for several temperatures. (b) The real part of the measured ion conductivity at various fixed frequencies vs reciprocal temperature. Lines corresponding to theoretical fits of Eq. (5) using parameters from Table I.

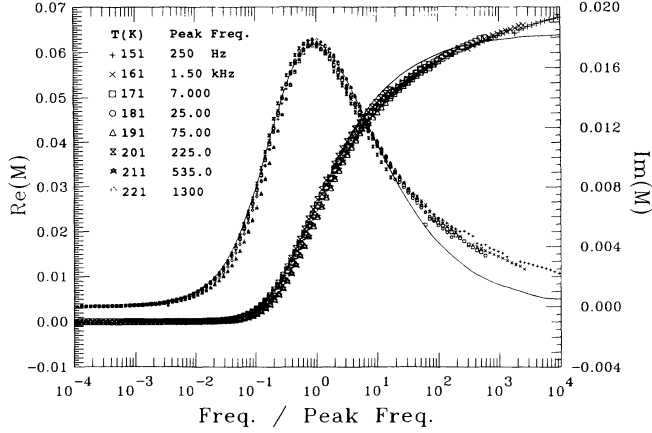


FIG. 2. The real and imaginary parts of the complex modulus vs a reduced frequency scale, frequency divided by peak frequency, where peak frequency is the frequency of the maximum in the imaginary part of the modulus. Solid lines represent theoretical fits of Eq. (4) using parameters from Table I.

This fast motion regime corresponds to the high- T side of the R_1 maximum shown in Fig. 3. Thus, in this temperature range, R_1 probes the long-time ($\omega\tau \ll 1$) behavior of the CF. It should be noted that if $f(t)$ can be represented as a weighted sum of exponential functions then the effective correlation time τ_{eff} becomes $\langle \tau \rangle$, the weighted average of the distribution of the corresponding correlation times.

In order to relate the ac conductivity to the dynamical properties of the diffusing ions, one can rely on the electric modulus formulation¹⁵ or on the generalized Nernst-Einstein formalism.¹⁶ Although the second approach relates more directly the conductivity to the frequency spectrum of hopping motion,¹⁷ the first approach, which is merely phenomenological, will be used here because it allows a more direct comparison of NMR and conductivity data. The ac conductivity can be expressed in terms of the electric modulus formulation¹⁵ by

$$\sigma(\omega) = \omega \epsilon_0 \epsilon''(\omega) = \omega \epsilon_0 M'' / (M'^2 + M''^2), \quad (3)$$

where M' and M'' are the real and imaginary parts of the electric modulus $M^*(\omega) = 1/\epsilon^*(\omega)$ and $\epsilon^*(\omega)$ is the complex dielectric constant. Since the electric modulus is related to the CF $\phi(t)$ describing the relaxation of the electric field by^{15,18,19}

$$M^*(\omega) = M_\infty \left[1 - \int_0^\infty dt \exp(-i\omega t) (-d\phi/dt) \right], \quad (4)$$

one has from Eqs. (3) and (4)

$$\sigma(\omega) = \frac{\epsilon_0 \epsilon_\infty 2 \int_0^\infty \cos(\omega t) \phi(t) dt}{\left[\int_0^\infty \sin(\omega t) \phi(t) dt \right]^2 + \left[\int_0^\infty \cos(\omega t) \phi(t) dt \right]^2}, \quad (5)$$

where ϵ_0 and $\epsilon_\infty = M_\infty^{-1}$ are the limiting values of the dielectric constant.

For $\omega \rightarrow 0$, one has for the dc conductivity

$$\sigma_{\text{dc}} = \epsilon_0 \epsilon_\infty \int_0^\infty \phi(t) dt = \epsilon_0 \epsilon_\infty / \tau_{\text{eff}} = \epsilon_0 \epsilon_\infty / \langle \tau \rangle, \quad (6)$$

where the last step in Eq. (6) is valid only if $\phi(t)$ can be represented as sum of exponentials, each having its own correlation time τ . Thus σ_{dc} also probes the long-time ($\omega\tau \ll 1$) behavior of the correlation function $\phi(t)$ and one expects

$$(R_1)_{\text{H-T}} \propto \sigma_{\text{dc}}^{-1} \quad (7)$$

where $(R_1)_{\text{H-T}}$ is the NSLR on the high-temperature side of the R_1 maximum. A more general relation between the NSLR and the conductivity is obtained from Eqs.

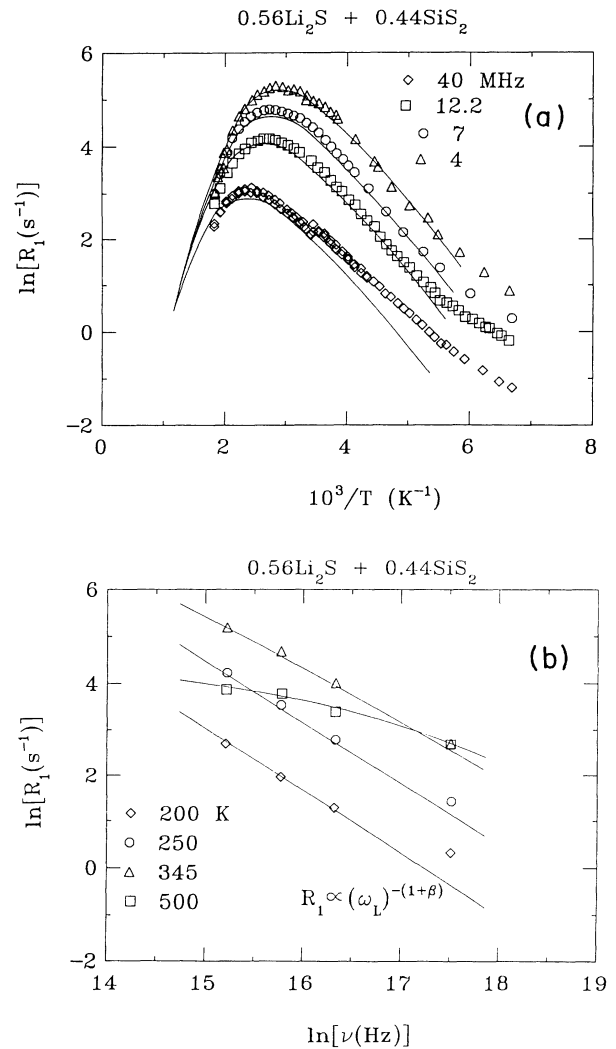


FIG. 3. ^7Li spin-lattice relaxation rate in $0.56\text{Li}_2\text{S} + 0.44\text{Si}_2\text{S}_2$. (a) Logarithm of the relaxation rates measured at 4, 7, 12.2, and 40 MHz as functions of reciprocal temperature $1000/T$ (K^{-1}). (b) Double-logarithmic plot of the relaxation rate vs measuring frequency. The straight line represents the limiting behavior according to Eq. (10b) for $\beta = 0.35$ (see Table I). All lines in parts (a) and (b) are theoretical fit curves from Eqs. (1) and (9) with the parameters in Table I. The interaction constant in Eq. (1) is $C = 3.8 \times 10^9$ ($\text{rad sec})^{-2}$.

(1)–(4):

$$R_1 \propto \frac{M''(\omega_L)}{\omega_L} + \frac{4M''(2\omega_L)}{2\omega_L}, \quad (8)$$

where ω_L is the NMR Larmor frequency and temperature T is the implicit parameter. Equations (7) and (8) depend on the electric modulus formalism chosen to describe $\sigma(\omega)$ but are otherwise independent of the model assumed for the correlation function; their validity implies that the time decay of $f(t)$ and $\phi(t)$ is due to the same mechanism and that the time dependence is the same.

In order to obtain quantitative information about relaxation and fluctuations from the combined NMR and conductivity measurements it is necessary to refer to a specific model for the time dependence of the relevant CF. The large asymmetry of the NSLR logarithmic plots vs reciprocal temperature in Fig. 3 and the frequency dependence of both R_1 and $\sigma(\omega)$ are indicative of strong nonexponential behavior of the correlation functions $\phi(t)$ and $f(t)$. The stretched-exponential function has been shown to offer an empirical way to model nonexponential relaxation phenomena in complex systems. Hence,

$$\phi(t) \propto f(t) \propto \exp(-t/\tau_c^*)^\beta \quad (9)$$

$$(a) \omega_L \tau_c^* \ll 1; R_1 \propto \tau_c^*; \sigma(\omega) \equiv \sigma_{dc} \propto (\tau_c^*)^{-1},$$

$$(b) \omega_L \tau_c^* \gg 1; R_1 \propto \omega_L^{-(1+\beta)} (\tau_c^*)^{-\beta}; \sigma(\omega) \propto \omega^{(1-\beta)} (\tau_c^*)^{-\beta}, \quad (10)$$

$$(c) \omega_L \tau_c^* = 0.64; (R_1)_{\max} \propto \exp(+E_A^*/kT_{\max}),$$

where conditions (a) and (b) correspond to the high- T side and low- T side of the R_1 maximum, respectively (see Fig. 3). The predictions of Eq. (10) are approximately borne out in the experimental results as shown in the figures confirming the general validity of a description of the NMR data in terms of a stretched-exponential correlation function.

The deviation of the NMR data from the curve of best fit [see Fig. 3(a)] could be due to an additional frequency-independent contribution to relaxation. The discrepancy becomes important only at low temperature and for high frequency. Analogous effects in ^7Li relaxation have been reported in other Li-based superionic glasses.^{20,21} It is possible the additional contribution is due to a two-phonon Raman process involving low-frequency phonon modes or local disorder modes. Such a contribution would add a BT² term at temperatures

with

$$\tau_c^* = \tau_0^* \exp(-E_A^*/kT),$$

where τ_c^* and E_A^* are an effective correlation time and an effective activation energy describing the microscopic Li^+ ion hopping dynamics.

The experimental data can be fit to the theoretical predictions (1) and (5) by using Eq. (9) for the CF. The parameters obtained from the fitting are summarized in Table I and the theoretical curves are shown in Figs. 1–3 together with the experimental data. It is important to note that, in partial contrast with previous reports, R_1 and $\sigma(\omega)$ have to be fitted with different values of $\beta_R = 0.35$ and $\beta_\sigma = 0.48$ (Table I). Equation (7) is approximately satisfied because the activation energies from $(R_1)_{\text{H-T}}$ and σ_{dc} data are approximately equal. However, Eq. (8) is not satisfied, since the β values describing $\phi(t)$ and $f(t)$ are different and therefore give rise to different frequency dependences of R_1 and $M''(\omega)$. Direct testing of Eq. (8) must await measurement of R_1 and $M''(\omega)$ over the same frequency range.

Using Eqs. (1), (5), and (9) the following limiting behavior should be observed in the NSLR and conductivity measurements:

below room temperature. The damping of the phonons due to Li diffusional motion should drastically reduce this contribution at high temperature.²¹ One should mention, however, the deviation of the experimental data from the theoretical fitting curves at low temperature and high frequency [Fig. 3(a)] could also indicate a shortcoming in the description of the CF in terms of a stretched exponential.

The deviation of $\sigma(\omega)$ from the theoretical curve at low temperature and high frequency is ascribed to the known failure of the KWW function at high frequency.¹⁵ To date there has not been a satisfactory explanation for this failure. It is not clear whether the function simply can not fit the data or whether there is an "extra" relaxation at high frequencies that contributes to $M''(\omega)$ keeping $M''(\omega)$ from going to zero as $\omega \rightarrow \infty$. In general, the more non-Debye like the conductivity, i.e., the more β deviates from unity, the greater the high-frequency failure of the KWW function. For example Patel and Martin²² have found that for $x \text{Na}_2\text{S} + (1-x) \text{B}_2\text{S}_3$ glasses, as β goes to unity for $x \rightarrow 0$ ($x \sim 0.001$), the KWW function shows an excellent fit to the M'' and M' data over five decades of frequency. On the other hand Mangian and Johan²³ have recently observed with highly doped, high conductivity $x \text{AgI} + (1-x) \text{AgPO}_3$ glasses, $\beta \sim 0.5$ and large deviations of the M'' and M' curves

TABLE I. Values of the parameters for KWW function [see Eq. (9)] used to fit the experimental data in Figs. 1–3.

	β	E_A^* (K)	τ_0^* (sec)
Conductivity	0.48	4000±50	4.0×10^{-15}
NMR	0.35	4500±200	4.5×10^{-14}

from the KWW calculated curves were found.

The comparison of the NMR and conductivity data has been considered by others,^{2,5,24} but not in cases where the behavior could be tested over wide ranges of both temperature and frequency as is done here, thus leading to a fortuitous agreement between the two β values. The differences found here for the values of β and τ_0^* from $\sigma(\omega)$ and NMR (Table I) implies a different time dependence of the CF's. Let us first discuss the observed difference between NMR and conductivity in terms of an homogeneous correlation function. The CF $\phi(t)$ in Eq. (5) refers to the relaxation of the electric field, which is a macroscopic quantity at $q=0$, i.e.,

$$\phi(t) \propto \langle E_{q=0}(t)E_{q=0}(0) \rangle,$$

while $f(t)$ in Eq. (1) is a local CF and is thus the result of collective fluctuations at *all* q vectors, i.e.,

$$f(t) \propto \langle u_i(t)u_j(0) \rangle \propto \Sigma_q \langle V_q(t)V_{-q}(0) \rangle,$$

where u_i is a local atomic coordinate.²⁵ In the presence of cooperative effects in ionic diffusion, the relaxation of the collective modes can be different for the various q values, thus leading to different time dependences of $\phi(t)$ and $f(t)$ as inferred here, and in particular τ_0^* values differing an order of magnitude.

A homogeneous CF displaying the KWW functional behavior can be obtained from a number of models.^{9,17,26} In particular, the semiphenomenological coupling model⁹ predicts a cross-over time $t_c = \omega_c^{-1}$, which separates an initial fast exponential decay of the CF driven by "single particle" dynamics from a slower decay at longer times described by the stretched exponential and related to cooperative effects. In the jump relaxation model,¹⁷ the slowing down of the CF at long times is explained by the presence of preferred occurrence of backwards hops following the first hop of the given ion. It can be argued that the correlation between successive hops should affect in different ways the local NMR CF, $f(t)$ and the conductivity CF $\phi(t)$, thus leading to different β values. The difference between β_σ and β_R should then be useful in learning about the nature of the cooperative behavior if a theory can be developed that relates quantitatively the value of β to the microscopic parameters.

An alternative approach consists in describing both $R_1(\omega)$ and $\sigma(\omega)$ with a random hopping model with a wide distribution of activation energies. In this case one has to fit both $R_1(\omega)$ and $\sigma(\omega)$ by using the same distribution function. A model to describe the conductivity in the presence of a distribution of barriers obtained as a simple extension of the Debye model appears to yield satisfactory results.²⁷ Within the framework of this microscopic model, the difference of β_R and β_σ can be viewed simply as a different way in which the distribution of barriers affects the fluctuations $R_1(\omega)$ and the relaxation $\sigma(\omega)$.

From the experimental viewpoint, the analysis of

NMR and $\sigma(\omega)$ data presented here should be extended to superionic systems having even greater ionic mobility and to conductivity frequencies that overlap those of NMR so as to allow studies over large and overlapping domains of frequency and temperature.

IV. SUMMARY AND CONCLUSIONS

In this work, the relationship between the fluctuation driven ⁷Li nuclear spin-lattice relaxation rate and the relaxation driven lithium ionic conductivity in fast-ionically-conducting Li₂S+SiS₂ glasses have been examined over wide ranges of frequency and temperature. Measurements of the conductivity have been made from 100 to 500 K and from 1 Hz to 3.76 MHz. Measurements of the ⁷Li spin-lattice relaxation rates have been measured at 4, 7, 12, and 40 MHz over the temperature range 100–500 K. Both processes were observed to be highly nonexponential in nature and the extent of nonexponentiality was quantified using the stretched-exponential Kohlrausch-Williams-Watts function. Both processes were accurately modeled using the KWW function, although different β parameters, $\beta_R=0.35$ and $\beta_\sigma=0.48$ were required to fit the data. The activation energies were likewise found to be slightly different, $E_{AR}=4500\pm 200$ K and $E_{A\sigma}=4000\pm 50$ K. An order-of-magnitude difference was found with this analysis method, in the pre-exponential factors, $\tau_{0R}=4.5\times 10^{-14}$ sec and $\tau_{0\sigma}=4\times 10^{-15}$ sec. These differences, although unexpected from the outset, were used to suggest the dynamics of the fluctuation driven spin-lattice relaxation rate and the relaxation driven ionic conductivity are different in detail but have gross features in common. In particular, we suggested such differences persist in the presence of cooperative ion dynamics but can be eliminated in the limit of no cooperative motions. This hypothesis will be tested in future work by examining low alkali-metal content glasses where cooperative effects between the cations can be reduced in the limit of infinite dilution.

ACKNOWLEDGMENTS

The authors thank M. Trunnell and H. Wang for assisting with the relaxation measurements, and in computer fitting of the experimental data, and Professor I. Svare for many stimulating discussions. Ames Laboratory is operated for the U.S. Department of Energy by Iowa State University under Contract No. W-7405-Eng-82. This work was supported by the Director of Energy Research, Office of Basic Energy Sciences (F.B. and D.R.T.), and by NSF-DMR Grant Nos. 87-01077 and 91-04460, Iowa State University Achievement and Research Foundation (S.W.M. and H.K.P.). Partial support by NATO Grant No. 0034/90 is gratefully acknowledged.

- *Also at Dipartimento di Fisica, University of Pavia, Pavia, Italy.
- ¹D. Brinkmann, *Solid State Ionics* **5**, 53 (1981).
- ²S. Martin, *Mater. Chem. Phys.* **23**, 225 (1989), and references therein.
- ³C. A. Angell, *Solid State Ionics* **18/19**, 72 (1985).
- ⁴K. L. Ngai, *Comments Solid State Phys.* **9**, 127 (1979); **9**, 141 (1980).
- ⁵C. A. Angell and S. W. Martin, in *Solid State Ionics*, edited by G. Nazri, R. A. Huggins, and D. F. Shriver, MRS Symposia Proceedings No. 135 (Materials Research Society, Pittsburgh, 1989), p. 73.
- ⁶M. Villa and J. L. Björkstam, *Solid State Ionics* **9/10**, 1421 (1983); J. L. Björkstam, J. Listerud, and M. Villa, *ibid.* **18/19**, 117 (1986); see also S. H. Chung, K. R. Jeffery, J. R. Stevens, and L. Borjesson, *Phys. Rev. B* **41**, 6154 (1990).
- ⁷R. Kolrausch, *Ann. Phys. (Leipzig)* **91**, 56 (1854); **91**, 179 (1854); G. Williams and D. C. Watts, *Trans. Faraday Soc.* **66**, 80 (1970).
- ⁸C. P. Lindsey and G. D. Patterson, *J. Chem. Phys.* **73**, 3348 (1980).
- ⁹K. L. Ngai, R. W. Rendell, A. K. Rajagopal, and S. Teitler, *Ann. N.Y. Acad. Sci.* **484**, 150 (1986); **484**, 321 (1986).
- ¹⁰S. W. Martin, H. K. Patel, F. Borsa, and D. R. Torgeson, *J. Non-Cryst. Solids* **131-133**, 1041 (1991).
- ¹¹J. A. Sills, M.S. thesis, Iowa State University, 1990.
- ¹²H. K. Patel, M.S. thesis, Iowa State University, 1989.
- ¹³The NMR spectrometer employed a programmable pulse sequencer: D. J. Adduci and B. C. Gerstein, *Rev. Sci. Instrum.* **50**, 1403 (1979); a double sideband rf switch: D. R. Torgeson and D. J. Adduci (unpublished).
- ¹⁴A. Pradel and M. Ribes, *Mater. Chem. Phys.* **23**, 121 (1989).
- ¹⁵P. B. Macedo, C. T. Moynihan, and R. Bose, *Phys. Chem. Glasses* **13**, 171 (1972); V. Provenzano, L. P. Boesch, V. Volterra, C. T. Moynihan, and P. B. Macedo, *J. Am. Ceram. Soc.* **55**, 492 (1972).
- ¹⁶W. Schirmacher, *Solid State Ionics* **28/30**, 129 (1988).
- ¹⁷K. Funke and R. Hoppe, *Solid State Ionics* **40/41**, 200 (1990), and references therein.
- ¹⁸K. L. Ngai, J. N. Mundy, H. G. Jain, O. Kanert, and G. Balzer-Jöllenebeck, *Phys. Rev.* **39**, 6169 (1989).
- ¹⁹Equation (4) is the same as the relation between the dielectric tensor $\epsilon(q, \omega)$ and the polarization correlation function, see E. L. Pollock and B. J. Alder, *Phys. Rev. Lett.* **46**, 950 (1981).
- ²⁰M. Grüne, H. Meierkord, W. Muller-Warmuth, P. Zum Hebel, B. Krebs, and M. Wulff, *Ber. Bunsenges. Phys. Chem.* **93**, 1313 (1989).
- ²¹M. Trunnell, D. R. Torgeson, S. Martin, and F. Borsa, *J. Non-Cryst. Solids* **139**, 257 (1992).
- ²²H. K. Patel and S. W. Martin, *Phys. Rev. B* **45**, 10292 (1992).
- ²³M. B. M. Mangian and G. P. Johan, *Phys. Chem. Glasses* **29**, 225 (1988).
- ²⁴G. Balzer-Jöllenebeck, O. Kanert, H. Jain, and K. L. Ngai, *Phys. Rev. B* **39**, 6071 (1989).
- ²⁵F. Borsa and A. Rigamonti, in *Magnetic Resonance of Phase Transitions*, edited by F. J. Owens, C. P. Poole, and H. A. Farach (Academic, New York, 1979).
- ²⁶S. R. Elliott and A. P. Owens, *Phys. Rev. B* **44**, 47 (1991).
- ²⁷I. Svare, D. R. Torgeson, S. Martin, and F. Borsa (unpublished).